

BOOSTING THE MAGNETIC FIELD OF A TOROIDAL CONDUCTIVE FLUID BY A POLOIDAL FLOW

Mamoru Otsuki*

Independent researcher

ORCID: 000-0002-5878-1300

*e-mail: gangankeisun@nifty.com

Abstract Cowling's theorem asserts that applying the first-order derivative of the stream function of the magnetic field results in a value of zero and its second-order derivative does not result in a value of zero. Thus, a contradiction to the magnetic maximum or minimum pole in the electromagnetic induction equation occurs. However, a different interpretation of this assertion is presented in this paper. If Ohm's law in Cowling's theorem includes an electromotive force due to a vector potential, this equation can be satisfied, which is why the magnetic flux fluctuates. The self-excitation mechanism causes these fluctuations. In this paper, a theory that decomposes vector potential into inductance and current is introduced, and it is solved as an eigenvalue problem. Considering the suppression of convection by the Lorentz force is equally essential to understanding the stability of the magnetic fields.

Keywords: Poloidal flow, dynamo theory, electromagnetic induction, inductance, conductive fluid, magnetohydrodynamics

1. INTRODUCTION

Cowling's theorem [1] states that axisymmetric magnetic fields are not maintained in the axisymmetric convection of conductive fluids. Some of the reasons for this are as follows. The first-order derivative of the stream function of the magnetic field is zero, and its second-order derivative is not zero. Applying these results to the magnetic maximum or minimum pole (hereafter abbreviated as pole) causes a contradiction in the

electromagnetic induction equation. However, a different interpretation of this assertion is presented in this paper.

Unless otherwise explained, symbols or similar symbols with the same meaning as in Cowling's theorem are used in this chapter only. In Cowling's theorem, Equation (2) does not include an electromotive force due to the vector potential calculated through Ohm's law.

$$J = \sigma(c_{\wedge} \mathbf{H} - \text{grad } V)$$

It is added as shown below.

$$J = \sigma \left(c_{\wedge} \mathbf{H} - \frac{1}{\omega} \frac{\partial \psi}{\partial t} - \text{grad } V \right)$$

Reflecting this in the electromagnetic induction equation and organizing it yields the following:

$$\frac{\partial \psi}{\partial t} = \frac{1}{\sigma \mu_0} \left(\frac{\partial^2 \psi}{\partial \omega^2} + \frac{\partial^2 \psi}{\partial z^2} - \frac{1}{\omega} \frac{\partial \psi}{\partial \omega} \right) + \frac{1}{\omega} \left(\frac{\partial \psi}{\partial \omega} \frac{\partial \phi}{\partial z} + \frac{\partial \phi}{\partial \omega} \frac{\partial \psi}{\partial z} \right) \quad (\text{c1})$$

What happens if we substitute $\frac{\partial \psi}{\partial \omega} = 0$, $\frac{\partial \psi}{\partial z} = 0$, $\frac{\partial^2 \psi}{\partial z^2} \neq 0$ and $\frac{\partial^2 \psi}{\partial \omega^2} \neq 0$ in this equation? Of course, the right side does not become zero, and the left side fluctuates. That is, even if there is a specific pole and its second-order derivative value is not zero, this equation is satisfied.

It can be understood that the magnetic flux decreases due to attenuation according to the first term on the right side. If the contradiction can be eliminated in this way in terms of a specific pole in attenuation, there will be no contradiction even if the magnetic flux increases. For example, a mechanism that acts like a negative resistance ($\sigma < 0$ for conductivity) is considered equivalently. Therefore, a self-excitation mechanism will be considered later.

However, even if such a thing were to happen, it would be unreasonable to unilaterally increase it. We must think that in the long run, it will either stop or vibrate. This needs to be examined dynamically, but this is not the scope of this study. However, the stability of the magnetic field can be maintained by the suppression of convection by the Lorentz force. This is because in the case of convection of moderate strength, when the current grows significantly, convection is suppressed by the Lorentz force.

As an example, the self-excitation mechanism is explained in detail below using a numerical calculation that decomposes the vector potential into inductance and current. In addition, the numerical calculation results are also introduced.

The inductance is important for understanding this example. Here, an overview of how inductance is handled is described. As an axisymmetric convection, poloidal convection is considered. Since it is a convection of a conductive fluid, it is thought that multiple coaxially toroidal circular electrical circuits (hereinafter referred to as coils) move as a bundle in a poloidal manner. The inductance referred to above is the inductance of these coils. It refers to both the self-inductance and mutual inductance between the coils.

When the coil moves in a poloidal manner, the coil moves in the radial direction and the cylindrical axial direction of the cylindrical coordinates. Then, the coil crosses the existing magnetic field and generates electricity. This power generation is self-excited, and it is solved as an eigenvalue problem.

1. MECHANISM

2.1 Description of the problem

To determine whether a magnetic field can fluctuate in the poloidal stream of a conductive fluid, a certain poloidal flow is set, and the induction equation (as a simultaneous equation expressed by inductances) is expressed in terms of toroidal vector potentials to calculate the current as an eigenvalue problem. The poloidal flow of a fluid occurs in a torus shape, as shown in Fig. 1, where U is the poloidal velocity, R_0 is the radius of the poloidal flow, and r is the radius of an example point on the torus from the Z axis. There are an infinite number of coils in the coil bundle. Here, only a part of the coils shown below will be considered.

A representative cross-section of the torus (Y - Z plane in Fig. 1) is shown in Fig. 2(a). The stream is divided into toroidal segments for calculation as coils (Fig. 2(b)). In this figure, Z is the center axis, and R_a is the radial axis of the cylindrical coordinates (equivalent to the Y axis in Fig. 1), where the circle indicates the cross-section of the torus. P_c is the center of the flow, where r_0 and z_0 are the elements of position P_c in the R_a and Z directions, respectively. Notably, z_0 is at the coordinates $(0,0)$, and P_c is at $(r_0,0)$. In Fig. 2(a), P is a representative position at which the flow velocity vector U is calculated; u_r and u_z are the elements of U in the R_a and Z directions, respectively; φ is an angle between the R_a axis and Point P ; and r is the element of Point P in the R_a direction. Fig. 2(b) shows the definition of the coils used to define the flow torus. Sixteen coils are considered, where n refers to the coil number. The dotted lines indicate the coaxial coils (i.e., the region occupied by the fluid), which are separated by the thickness T . There are multiple coils that wind only once around the Z axis, and the coils move in the direction of U with radius R_0 . Electric current runs separately in each coil in the θ direction that orbits the Z axis.

Although the coils can move, the later calculation of the eigenvalues assumes the state of the coils in a brief moment, Δt .

Figs. 3(a) and (b) show the top and side views, respectively, of a set of any two of the coaxial coils shown in Fig. 2 to explain the relationship between the electric current (I) and vector potential (\mathbf{A}). In addition, a 3D image of the coils is shown in Fig. 4 to clarify their relationship with each other. Each coil is arrayed coaxially with the Z axis, and they are parallel to each other. X, Y, and Z are the axes of the rectangular Cartesian coordinate system shown in Fig. 3. C_j is Coil j , in which the current I_j flows, and C_i is Coil i , which obtains the vector potential A_j induced by the current I_j running in Coil C_j . θ is the angle of rotation around the Z axis, starting from the Y axis. Here, r_i and r_j are the radii of C_i and C_j , respectively. Furthermore, ds_i and ds_j are minute lengths of C_i and C_j for integration, respectively, where ds_i is placed on the X axis ($\theta = 0$), and ds_j is placed at θ with a distance l between them to define the range of the integral. $I ds_j$ is the contribution to the current over ds_j , where $A ds_j$ is the vector potential induced by $I ds_j$. dA_j is the element of $A ds_j$ in the X direction, and it is integrated with respect to θ to obtain A_j . Φ_i is the total flux linking C_i .

1.2 Calculation of the magnetic properties

To determine the fluctuation in the magnetic field in the coils described in the previous section, the current is calculated using Ohm's law with the electric field [2].

$$\mathbf{J} = \sigma(\mathbf{E} + \mathbf{u} \times \mathbf{B}) \quad (1)$$

Here, \mathbf{J} is the current density; σ is the electric conductivity; \mathbf{u} is the velocity of the conductive fluid; and \mathbf{B} is the magnetic field, which can be found using Eq. (2); $\mathbf{u} \times \mathbf{B}$ is

the motion of the electric field; and E is the electric field potential, which can be found using Eq. (3).

$$\mathbf{B} = \nabla \times \mathbf{A} \quad (2)$$

$$\mathbf{E} = -\frac{\partial A}{\partial t} + \nabla \varphi' \quad (3)$$

Here, φ' is a scalar potential, A is a vector potential, and t represents the time.

To derive an induction equation expressed in vector potentials from Ohm's law, these equations are combined as follows.

$$\frac{\partial A}{\partial t} - \mathbf{u} \times (\nabla \times \mathbf{A}) = \nabla \varphi' - \frac{I}{\sigma} \quad (4)$$

To apply this induction equation for coils, the factor $2\pi r$ (r = coil radius) is multiplied as an integral around the coil on both sides of the equation because the current is the same around C_j . Assuming $\mathbf{J} = I/S$, where I is the toroidal current and S is the cross-sectional area of the coil, Eq. (4) can be rewritten as follows:

$$\frac{\partial}{\partial t} (2\pi r_i \mathbf{A}) - \mathbf{u} \times (\nabla \times 2\pi r_i \mathbf{A}) = -\frac{2\pi r_i I}{\sigma S} \quad (5)$$

Here, φ' is ignored because it is assumed that going around along C_i at that gradient will result in a value of zero. Furthermore, Eq. (6) shows the relationship between A and the inductance L [3]. Here, the total magnetic flux linking the coil, Φ , is used in place of L , where $\Phi = LI$. The subscripts i and j refer to the coil numbers defined in Fig. 2, enabling the development of simultaneous equations.

$$\Phi_i = \oint_{C_i} \mathbf{A}_j ds_i \quad (6)$$

Here, Φ_i is the flux of Coil C_i , and ds_i is a minute part of Coil C_i .

In this arrangement of coils, all the coils are arrayed coaxially with the Z axis and parallel to each other. Thus, A_j is the same around C_i . Therefore, $\Phi_i = 2\pi r_i A_j$ when $\Phi_i = L_{ij} I_j$. Then,

the relationship between L_{ij} and A_j is as follows. L_{ij} is a matrix that represents the inductance. Only the diagonal element represents the self-inductance, and the other elements represent the mutual inductance. Thus, it is hereafter referred to as M_{ij} .

$$\mathbf{A}_j = \frac{I_j}{2\pi r_i} M_{ij} \quad (7)$$

As will be discussed later, both \mathbf{A}_j and I_j have only a toroidal component along the coil.

By substituting Eq. (7) into Eq. (5), the following equation is obtained.

$$\frac{\partial}{\partial t} (M_{ij} I_j) - \mathbf{u} \times (\nabla \times 2\pi r_i \mathbf{A}_j) = -\frac{2\pi r_i}{\sigma S} I_j \quad (8)$$

Here, σ is the conductance of the fluid, and r_i is the radius from the Z axis. However, the second term on the left-hand side of Eq. (8) is complicated. Thus, it must be addressed separately. It is considered by decomposing the term as follows.

$$\begin{aligned} \mathbf{u} \times (\nabla \times \mathbf{A}_j) &= \begin{bmatrix} u_{ir} \\ 0 \\ u_{iz} \end{bmatrix} \times \begin{bmatrix} \frac{1}{r_i} \left(-r_i \frac{\partial A_{j\theta}}{\partial z_i} \right) \\ 0 \\ \frac{1}{r_i} \left(\frac{\partial r_i A_{j\theta}}{\partial r_i} \right) \end{bmatrix} = \begin{bmatrix} u_{ir} \\ 0 \\ u_{iz} \end{bmatrix} \times \begin{bmatrix} -\frac{\partial A_{j\theta}}{\partial z_i} \\ 0 \\ \frac{1}{r_i} A_{j\theta} + \frac{\partial A_{j\theta}}{\partial r_i} \end{bmatrix} = \\ & \begin{bmatrix} 0 \\ -u_{iz} \frac{\partial A_{j\theta}}{\partial z_i} - u_{ir} \left(\frac{1}{r_i} A_{j\theta} + \frac{\partial A_{j\theta}}{\partial r_i} \right) \\ 0 \end{bmatrix} \end{aligned} \quad (9)$$

Here, $\text{rot} \mathbf{A}_j$ is decomposed into cylindrical coordinates, and Subscripts r , θ , and z indicate the component directions in the cylindrical coordinates, namely, the radius from the Z axis, the angle around the Z axis, and the Z direction, respectively. Then, since the current only runs through the toroidal coil, only the toroidal $A_{j\theta}$ component remains with the vector potential. Furthermore, since it is uniform in the toroidal direction, the $\frac{\partial}{\partial \theta}$ component is zero, and the description is excluded. Therefore, A_j has a component that is

only in the θ direction. Thus, the other components of \mathbf{A}_j are omitted. Eq. (10) is obtained by multiplying Eq. (9) by $2\pi r_i$, substituting Eq. (7) and including only the θ component.

$$2\pi r_i \left[-u_{iz} \frac{\partial \mathbf{A}_{j\theta}}{\partial z_i} - u_{ir} \left(\frac{1}{r_i} \mathbf{A}_{j\theta} + \frac{\partial \mathbf{A}_{j\theta}}{\partial r_i} \right) \right] = -u_{iz} \frac{\partial M_{ij} I_{j\theta}}{\partial z_i} - u_{ir} \left(\frac{1}{r_i} M_{ij} I_{j\theta} + \frac{\partial M_{ij} I_{j\theta}}{\partial r_i} \right)$$

$$= -u_{ir} \frac{\partial M_{ij} I_{j\theta}}{\partial r_i} - u_{iz} \frac{\partial M_{ij} I_{j\theta}}{\partial z_i} - u_{ir} \frac{1}{r_i} M_{ij} I_{j\theta} \quad (10)$$

This is replaced by the second term on the left-hand side of Eq. (8) to obtain Eq. (11).

$$\frac{\partial}{\partial t} (M_{ij} I_{j\theta}) - \left(-u_{ir} \frac{\partial M_{ij} I_{j\theta}}{\partial r_i} - u_{iz} \frac{\partial M_{ij} I_{j\theta}}{\partial z_i} - u_{ir} \frac{1}{r_i} M_{ij} I_{j\theta} \right) = -\frac{2\pi r_i}{\sigma S} I_{j\theta} \quad (11)$$

$$\frac{\partial}{\partial t} (M_{ij} I_{j\theta}) + u_{ir} \frac{\partial M_{ij} I_{j\theta}}{\partial r_i} + u_{iz} \frac{\partial M_{ij} I_{j\theta}}{\partial z_i} + u_{ir} \frac{1}{r_i} M_{ij} I_{j\theta} = -\frac{2\pi r_i}{\sigma S} I_{j\theta} \quad (12)$$

The fourth term on the left side becomes rapidly weak when moving away from the cylindrical axis, so it will be omitted hereafter. Since the first three terms on the left-hand side of Eq. (12) are equivalent to a total differential, they can be replaced as follows:

$$\frac{d}{dt} (M_{ij} I_{j\theta}) = -\frac{2\pi r_i}{\sigma S} I_{j\theta}$$

When the equation is transformed and arranged, Eq. (13) is obtained.

$$\frac{dM_{ij}}{dt} I_{j\theta} + M_{ij} \frac{dI_{j\theta}}{dt} = -\frac{2\pi r_i}{\sigma S} I_{j\theta}$$

$$\frac{dI_{j\theta}}{dt} = M_{ij}^{-1} \left(-\frac{dM_{ij}}{dt} I_{j\theta} - \frac{2\pi r_i}{\sigma S} I_{j\theta} \right)$$

$$\Lambda I_{j\theta} = -M_{ij}^{-1} \frac{dM_{ij}}{dt} I_{j\theta} - M_{ij}^{-1} R_{ij} I_{j\theta} \quad (13)$$

Here, Λ indicates the eigenvalues. These simultaneous equations are used here to obtain the Λ values. R_{ij} is a matrix of the resistance and a function of the coil's

circumference and cross-sectional area S , where S is calculated from the thickness T and the section of the flow course as $S = (2\pi R_0 T)/16$. Then, $R_{ij} = 2\pi r_i / (\sigma S) = (16r_i)/(\sigma R_0 T)$. R_{ij} is a diagonal matrix because the voltage drop exists only for $i = j$.

The inductance used in the example calculation is as follows. In the coil description shown in Fig. 2, the coil's cross-sectional area and shape are disregarded in the calculation of the inductance because these geometrical factors introduce a large degree of complexity. Therefore, the coil is treated as a thin line as an approximation in Figs. 3(a) and (b). Subsequently, A_j is calculated as follows [2]:

$$A_j = \frac{\mu}{4\pi} \oint_{C_j} \frac{I}{l} dV = \frac{\mu}{4\pi} \oint_{C_j} \frac{IS}{l} ds_j = \frac{\mu}{4\pi} \oint_{C_j} \frac{I_j}{l} \cos \theta ds_j = \frac{\mu}{4\pi} I_j \oint_{C_j} \frac{\cos \theta}{l} ds_j, \quad (14)$$

where l is the distance between ds_i and ds_j , μ is the magnetic permeability, dV is the minute volume, S is the cross-sectional area of the current (i.e., the coil), $I_j = JS$ is the current, and the directional element for ds_i of I_j is $I_j \cos \theta$. When Eq. (7) is substituted for A_j in Eq. (14). Eq. (15) can be obtained.

$$M_{ij} = \frac{2\pi r_i}{I_j} \frac{\mu}{4\pi} I_j \oint_{C_j} \frac{\cos \theta}{l} ds_j = 2\pi r_i \frac{\mu}{4\pi} \oint_{C_j} \frac{\cos \theta}{l} ds_j \quad (15)$$

Here, Figs. 3(a) and (b) and Eq. (15) are used to explain the tendency of the inductance changing due to convection. Since the variable z_i is not included in Eq. (15), M_{ij} changes only with r_i . Therefore, the inductances change only due to the movement in the Y (Ra) direction of the convection, and there is no change in the Z direction. The fact that the coil crosses the existing magnetic field and generates power is due to a change in inductance. Therefore, power generation occurs only by the radial movement of convection. Notably, z_i is contained in Eq. (18). l_k will be described later. However, it cannot be modified in the partial derivative of the inductance. This is because the

partial derivative has a principle that does not change anything other than the target variable, so the pair of mutual inductance cannot be changed.

When μ is set to $4\pi \times 10^{-7}$ H/m (vacuum conditions), Eq. (16) is obtained.

$$M_{ij} = 2\pi r_i \oint_{C_j} \frac{\cos \theta}{l} ds_j \times 10^{-7} \quad (16)$$

M_{ij} is calculated by summation, where C_j is divided into $k = 100$ equal parts, Δs_j , as follows.

$$M_{ij} \doteq 2\pi r_i \sum_{k=1}^{100} \frac{\cos \theta_k \Delta s_j}{l_k} \times 10^{-7} \quad (17)$$

$$l_k = \sqrt{(r_i \cos \theta_k - r_j)^2 + (r_i \sin \theta_k)^2 + (z_i - z_j)^2} \quad (18)$$

The angle of a specific coil, n , is given by $\varphi_n = 2\pi n/16$, as shown in Fig. 2, where $r_n = r_0 + R_0 \cos \varphi_n$ and $z_n = R_0 \sin \varphi_n$. Earlier, i and j were used in the mutual inductance calculations to distinguish between the coils that received electromotive force and the coils that had a current flow. Each number n is replaced by i or j for any two of the coils. Here, $(\dot{\quad})$ is the same as $\frac{d}{dt}$. \dot{M}_{ij} is calculated as the difference in M_{ij} induced by the flow velocity over a period of a minute, divided by Δt (ex. 1.0×10^{-6} s). The velocity \mathbf{U} shown in Fig. 2 depends on the φ_n of each coil and is calculated as follows:

$$|\mathbf{U}| = \frac{r_0}{r_i} \omega R_0, u_r = -|\mathbf{U}| \sin \varphi_n, u_z = |\mathbf{U}| \cos \varphi_n, \quad (19)$$

where ω is the angular velocity of the flow. $\frac{r_0}{r_i}$ is a coefficient that adjusts based on the position of r_0 so that the flow rate satisfies the continuity equation.

Furthermore, M_{ij}^{-1} is the inverse matrix of M_{ij} .

3. DISCUSSION AND RESULTS

3.1. Discussion

Notably, Eq. (13) implies that the $-M_{ij}^{-1}\dot{M}_{ij}I_{j\theta}$ term may become positive (i.e., \dot{M}_{ij} becomes negative) because \dot{M}_{ij} depends on the velocity of the fluid. Therefore, the eigenvalue (Λ) is also dependent on the velocity, and some of the eigenvalues may be positive, i.e., eigenvectors that increase over time. The inductance M_{ij} in Eq. (15) is proportional to R_0 and r_0 because r_i , l , and ds originate from R_0 and r_0 . Therefore, \dot{M}_{ij} is also proportional to R_0 and r_0 . On the other hand, the $-M_{ij}^{-1}R_{ij}I_{j\theta}$ term is always negative and implies the attenuation of the eigenvalue. Furthermore, R_{ij} is inversely proportional to R_0 and r_0 because in the equation $R_{ij} = (16r_i)/(\sigma R_0 T)$, R_0 , T , and r_i originate from and are inversely proportional to R_0 and r_0 . Larger systems imply that the eigenvectors are less likely to attenuate. Since the effects of both above terms need to be viewed relatively, M_{ij}^{-1} in both sections is excluded. The above is clearly indicated by the results for the four presented conditions in the Results section.

Moreover, obtaining the eigenvalue under which the induction term exceeds the attenuation term is necessary to specifically understand the process. When the inductance of the coils changes by the flow velocity, the eigenvalues determined from Eq. (13) enable the interaction between the changes in the coil inductance and resistance to be shown as a fluctuation in the toroidal current. This result indicates a fluctuating magnetic field.

Some eigenvalues become positive under certain conditions, indicating that their eigenvector would increase over time. A positive eigenvalue exponentially increases its eigenvector (the current mode indicates each current in the coils; however, notably, its absolute value and polarity are not determined because of the character of their eigenvector). In contrast, a negative eigenvalue exponentially decreases its eigenvector.

However, a negative eigenvalue means a decrease in its eigenvector (attenuation of the current state) but does not reduce the eigenvector of other eigenvalues (for example, positive eigenvalues). Of course, this is only true in a case where each eigenvector is orthogonal. This calculation does not show perfect orthogonality; if the matrix on the right-hand side of Eq. (13) is separated into symmetric and alternating components, and the latter is not zero, imperfect orthogonality occurs. However, this is attributable to the coarse calculation. As a potential future work, numerical calculations are necessary to increase the order of the matrix and set the convection current over a wide area to evaluate the orthogonality of this system. However, this was beyond the scope of this theoretical contribution. Notably, even if the orthogonality is not perfect, the positive eigenvalues are expected to have some influence on the generated magnetic field. In the case of the large number of positive eigenvalues calculated in this study, it is expected that they would be dominant and increase the current eigenvector. The eigenvector of a negative eigenvalue is only influential if there is a current generated by the eigenvector of a positive eigenvalue. This can suppress the eigenvector with the positive eigenvalue but cannot reduce it to zero. Therefore, it is expected that the increasing trend in the eigenvector would be sustained by the positive eigenvalues, and the extent of this would depend on the specific conditions.

3.2. Results

Here, several eigenvalue case studies are described based on Eq. (13), as presented in the previous section. Four different cases are defined, as shown in Table 1. Table 2 lists the eigenvalues $\lambda(\lambda_1-\lambda_{16})$. Positive values contribute to the eigenvector increasing over

time, while negative values make it decrease over time. The positive values are highlighted in bold in the table. The general conditions assumed in the calculations of the eigenvalues were $\sigma = 1.0 \times 10^4$ S/m (based on typical plasma conductivity [4]) and $T=0.1R_0$.

In the case of Condition 1, λ_{16} is the λ value with the largest positive value, which implies that the eigenvector increases in magnitude over time. The number of positive eigenvalues depends on the size of the system and the flow velocity. Therefore, in the case of Condition 2, which has a higher ω than Condition 1 but the same system dimensions as Condition 1, three of the λ values are positive. Therefore, increasing the flow velocity causes the eigenvector magnitude to increase over time. In the case of Condition 3, which has a lower ω than Condition 1 but the same dimensions as Condition 1, all the λ values are negative. Therefore, the eigenvector magnitude would only decrease, and the magnetic field would not be sustained over time. In the case of Condition 4, the dimensions are an order larger than those in Condition 1. Because ω is an angular velocity, it scales proportionally. Thus, ω was decreased accordingly by an order of magnitude to make it comparable with that of Condition 1. In this case, three of the λ values are positive. Therefore, it is easy to increase the eigenvector magnitude over time (i.e., maintain a magnetic field) for larger systems.

In addition, Table 3 shows an eigenvector (a current mode) of the maximum eigenvalue in Condition 1. This condition indicates that the absolute value of the current is maximized in Coil 6, which is highlighted in bold. This means that the current increases exponentially with its eigenvalue as an exponent while maintaining this mode. The magnetic field due to this also increases. This magnetic field is rotationally symmetric

with the axis of the cylindrical coordinates, but the position of this current is different from the center of the convection. Thus, the magnetic flux path is different from the convection path, as shown in Fig. 5. However, this figure symbolically depicts the magnetic field due to the thin convection assumed in the calculation example.

4. CONCLUSION

Cowling's theorem states that the left side of Eq. (c1) should be zero for stability maintenance. Therefore, since the right side does not equal zero at the pole point, the axisymmetric magnetic field cannot be maintained because this equation cannot be satisfied. In my theory, this equation should include the electromotive force due to the vector potential. This leads to this equation showing that the magnetic field fluctuates. Since it fluctuates, it does not maintain stability, as Cowling's theorem suggests. However, my theory is that stability maintenance is achieved by the suppression of convection by the Lorentz force. Other theories do not have this viewpoint. To the best of the author's knowledge, this is a novel idea; in addition, there have been no other studies that calculated specific eigenvalues and showed how the magnetic field generation changed with the velocity of the fluid and the size of the system. Therefore, I think the calculation method presented here for illustration is equally useful.

The methodology presented here is relevant for conditions in which a poloidal axisymmetric magnetic field is generated. In the conductive fluid of a celestial body, poloidal convection may occur as a result of downflow due to a radial temperature gradient or chemical effects, as shown in Fig. 5. The sun and Earth have poloidal axisymmetric magnetic fields. However, the generation mechanism might be to some extent different from that assumed here. While this mechanism probably includes that

described here by the presented theory, for the moment, it is probably indistinguishable because it is mixed.

What about artificial systems such as liquid sodium and plasma furnaces? Since the scale is small, it seems to be disadvantageous in terms of scale. Considering the scale alone, it seems impossible to cause this phenomenon. However, if it is artificial, convection can be devised. For example, concentrate convection near the cylindrical axis can be achieved. Closer to the cylindrical axis, stronger induction is possible. In addition, if the convection is very close to the cylindrical axis, the term deleted from Eq. (12) may be affected. Therefore, this mechanism can still occur regardless of the small scale.

In this paper, calculations for a specific fluid flow (a thin layer of fluid under poloidal flow) are performed. The convection used in this paper is intended to provide a calculation example. If realistic convection is known, it can be calculated. Since the flow velocity can be set at any position, convection in a thin region, such as the convection shown here, is not necessary. In other words, axisymmetric and poloidal convection can be calculated by setting the convection to be distributed in an arbitrary region.

To apply this theory to real systems, it is necessary to consider the dynamics with respect to the Lorentz force and other factors [5]. To demonstrate the possibility and magnitude of the magnetic field generation as a function of the size and flow velocity of the system, the scale of the sun and its corresponding plasma conductivity were assumed here as a representative example. However, I think that the mathematics presented in this paper will be useful in studies regarding the sun, Earth and other celestial bodies, plasma furnaces, and sodium experiments.

Conflicts of interest.

The author has no conflicts of interest to declare.

Funding.

No funding was obtained for this work.

REFERENCES

1. T. G. Cowling and Q. J. Mech. Appl. Math. **10**(1), 129–136 (1957).
2. H. S. Reall, Mathematical Tripos Part IB: Electromagnetism [Internet]. Available from: www.damtp.cam.ac.uk/user/hsr1000/electromagnetism_lectures.pdf. Accessed 03/11/2022.
3. H. A. Haus and J. R. Melcher, *Vector Potential and the Boundary Value Point of View*. In: Electromagnetic Fields and Energy [Internet], Massachusetts Institute of Technology (1998). Available from: <https://ocw.mit.edu/courses/res-6-001-electromagnetic-fields-and-energy-spring-2008/pages/chapter-8/>. Accessed 03/11/2022.
4. A. Kanzawa, Netsu Bussei. **4**(1), 3-11 (1990) (In Japanese).
5. R. Stieglitz, Nonlin. Proc. Geophys. **9**, 165–170 (2002).

FIGURES

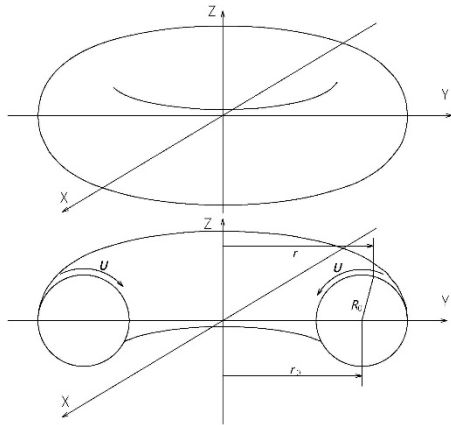


Fig. 1. Schematic of the toroidal geometry.

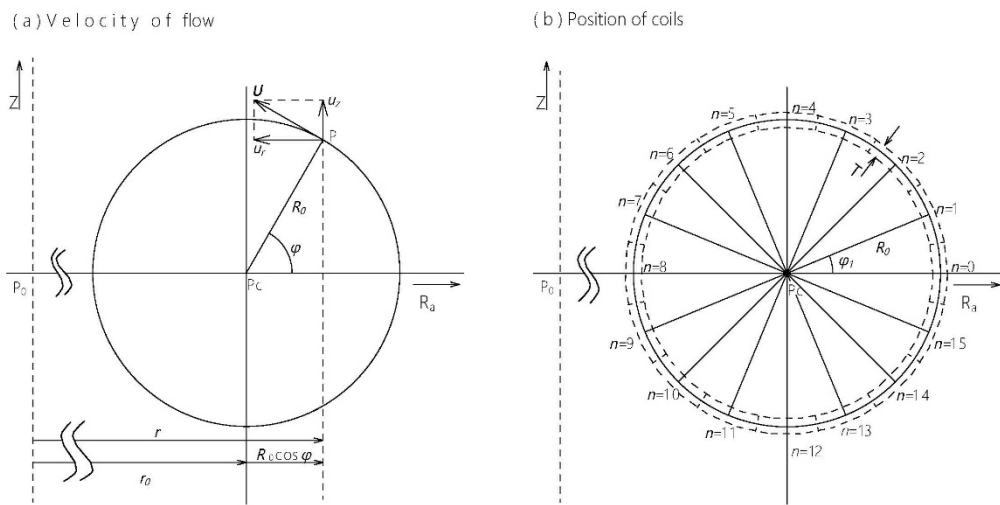


Fig. 2. Schematics of the (a) velocity of the fluid flow and (b) defined coils in the cross-section of the convection (Y–Z plane in Fig. 1).

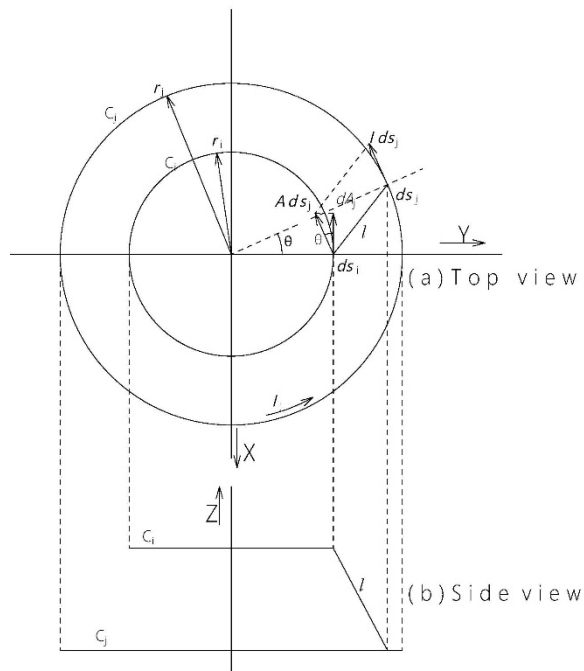


Fig. 3. Relationship between the electric current (I) and vector potential (A) for a set of any two coils shown in Fig. 2: (a) top view and (b) side view of the torus.

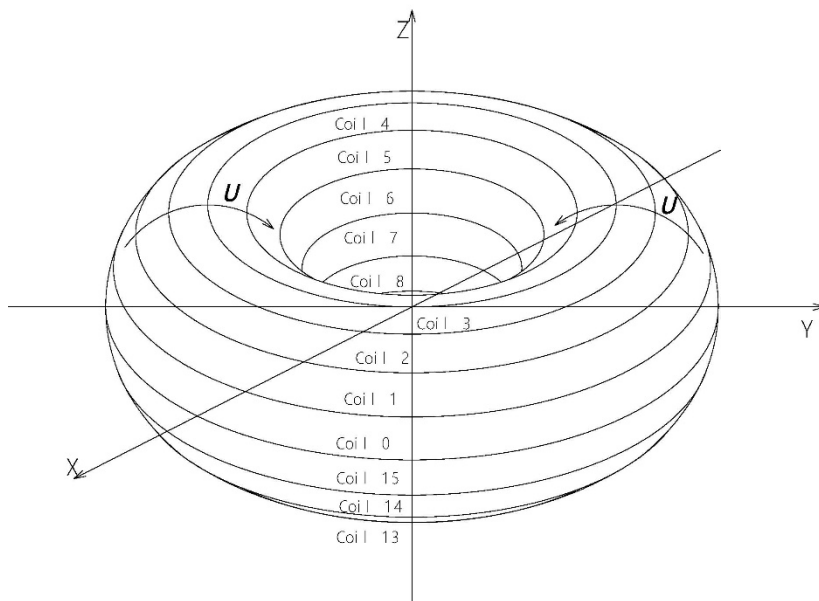


Fig. 4. 3D view of the coaxial coils.

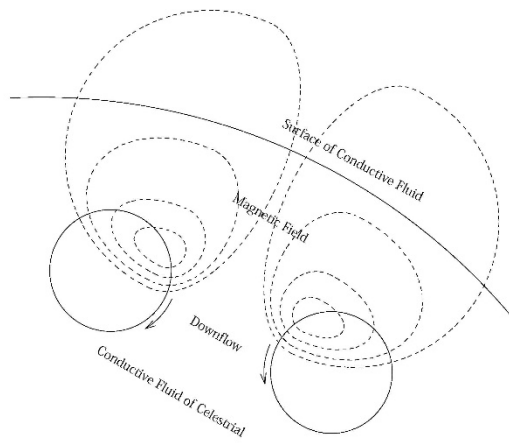


Fig. 5. Examples of the poloidal axisymmetric convection in a celestial body. The solid arrows indicate the fluid flow, while the dashed lines indicate the induced magnetic field.

FIGURES

Table 1. Definitions of the case conditions.

Condition	R ₀ (m)	r ₀ (m)	ω (rad/s)
1	1.0×10^3	2.0×10^3	$2\pi(3.0 \times 10^{-4})$
2	1.0×10^3	2.0×10^3	$2\pi(3.0 \times 10^{-3})$
3	1.0×10^3	2.0×10^3	$2\pi(2.0 \times 10^{-4})$
4	1.0×10^4	2.0×10^4	$2\pi(3.0 \times 10^{-5})$

Table 2. Eigenvalues λ of the four conditions shown in Table 1.

Eigenvalues	Condition 1	Condition 2	Condition 3	Condition 4
λ_1	-5.295×10^{-2}	-5.953×10^{-2}	-5.290×10^{-2}	-5.952×10^{-4}
λ_2	-3.228×10^{-2}	-3.852×10^{-2}	-3.224×10^{-2}	-3.852×10^{-4}
λ_3	-2.297×10^{-2}	-2.779×10^{-2}	-2.292×10^{-2}	-2.779×10^{-4}
λ_4	-1.770×10^{-2}	-2.757×10^{-2}	-1.766×10^{-2}	-2.757×10^{-4}
λ_5	-1.434×10^{-2}	-1.999×10^{-2}	-1.433×10^{-2}	-1.999×10^{-4}
λ_6	-1.203×10^{-2}	-1.449×10^{-2}	-1.205×10^{-2}	-1.449×10^{-4}
λ_7	-1.066×10^{-2}	-1.087×10^{-2}	-1.073×10^{-2}	-1.087×10^{-4}
λ_8	-8.974×10^{-3}	-1.022×10^{-2}	-9.006×10^{-3}	-1.022×10^{-4}
λ_9	-8.860×10^{-3}	-7.772×10^{-3}	-8.902×10^{-3}	-7.772×10^{-5}
λ_{10}	-6.559×10^{-3}	-6.767×10^{-3}	-6.481×10^{-3}	-6.767×10^{-5}
λ_{11}	-6.490×10^{-3}	-5.103×10^{-3}	-6.461×10^{-3}	-5.103×10^{-5}
λ_{12}	-5.036×10^{-3}	-3.838×10^{-3}	-4.539×10^{-3}	-3.838×10^{-5}
λ_{13}	-4.193×10^{-3}	-2.299×10^{-3}	-4.137×10^{-3}	-2.299×10^{-5}
λ_{14}	-3.101×10^{-3}	1.034×10^{-3}	-2.945×10^{-3}	1.034×10^{-5}
λ_{15}	-1.770×10^{-3}	3.203×10^{-3}	-1.864×10^{-3}	3.203×10^{-5}
λ_{16}	6.924×10^{-4}	2.332×10^{-2}	-3.298×10^{-5}	2.332×10^{-4}

Table 3. Eigenvector (Current Mode) of the Maxim Eigenvalue on Condition 1.

Coil numbers	Eigenvector (Current Mode)
0	4.844×10^{-2}
1	8.094×10^{-2}
2	1.300×10^{-1}
3	2.060×10^{-1}
4	3.193×10^{-1}
5	4.637×10^{-1}
6	5.711×10^{-1}
7	4.900×10^{-1}
8	2.006×10^{-1}
9	-1.664×10^{-2}
10	-6.302×10^{-2}
11	-4.861×10^{-2}
12	-2.820×10^{-2}
13	-1.005×10^{-2}
14	6.949×10^{-3}
15	2.535×10^{-2}